Heliyon 8 (2022) e08976

Contents lists available at ScienceDirect

Heliyon

journal homepage: www.cell.com/heliyon

Research article

Geophysical and contamination assessment of soil spatial variability for sustainable precision agriculture in Omu-Aran farm, Northcentral Nigeria

O.T. Kayode [a,*], A.P. Aizebeokhai [a], A.M. Odukoya [b]

[a] Department of Physics, College of Science and Technology, Covenant University, Ota, Nigeria
[b] Department of Geosciences, College of Science, University of Lagos, Nigeria

ARTICLE INFO

Keywords:
Electrical resistivity
Sustainable agriculture
Soil characterisation
Soil contamination
Omu-Aran
Nigeria

ABSTRACT

The spatial and temporal variability of soil properties (fluid composition, structure, and water content) and hydrogeological properties employed for sustainable precision agriculture can be obtained from geoelectrical resistivity methods. For sustainable precision agricultural practices, site-specific information is paramount, especially during the planting season. An integrated one-dimensional (1D) and two-dimensional (2D) electrical resistivity survey have been adopted to characterize the subsoil parameters and delineate the aquifer unit of large farm areas, especially in precision agricultural practices. Also, contamination assessment reveals the soil quality status of farmlands. This study aims to determine the site-specific soil parameters of a commercial farm in Omu-Aran, Northcentral, Nigeria. The subsoil features from the geoelectrical resistivity surveys indicate 3 to 4 distinctive lithology to a depth of 43.4 m into the subsurface of the farm. The ID (Vertical Electrical Sounding) and 2D resistivity inversion models results have revealed the heterogeneity nature of the topsoil, also known as the stone zone comprising of reworked clayey soil and sandy gravelly soil, the weathered/saprolite zone (gravelly sandy/sandy soil), the fractured basement and the fresh basement rock. Contamination factor (Cf), pollution load index (PLI) and Nemerow integrated pollution index (NIPI) were used to assess the contamination index on the farmland. Toxic elements such as arsenic, cadmium, chromium, cobalt, lead, manganese, nickel, and zinc have low to moderate contamination in the farm. The depth of investigation (≤3m) covers the upper root zone of significant crops grown in the area. The findings can assess soil contamination, delineate basement features, subsoil variability, soil profiling, and determine the subsoil hydrological properties.

1. Introduction

Soil as a natural medium that makes plants grow has variable soil properties in space and time. This change in soil properties is peculiar to every soil type; therefore, a continuous and precise spatial and temporal variation is essential. One of the commonly used geophysical methods to delineate subsoil features, aquifer geometry, determine the depth to aquifer units, and characterise the hydrological properties in groundwater exploration is the geoelectrical resistivity method [2]. This method has been used extensively by researchers for various soil investigations, hydrological and agricultural purposes [3, 8, 11, 14, 17, 18, 29, 34, 36, 39]. The heterogeneity of the area under investigation determines the type of survey to be performed (one-, two- or three-dimensional electrical resistivity survey) [36]. Therefore two-dimensional (2D) is ideal for agricultural investigations, giving both the lateral and soil profile of the farmland. The vertical electrical sounding (VES) is perfect for groundwater investigations. Groundwater has contributed immensely to irrigation agriculture, especially in the world's arid regions, and has become an essential part of economic development [20, 37]. Shakoor et al., [38] has reported that irrigated agriculture produces more than 60 percent of grain globally, contributing to groundwater resources.

The accumulation of potentially toxic metals into agricultural soils has increased significantly due to increased population and industrialization [44, 45]. Heavy metals accumulate in the soil through human-induced and natural processes. Parent materials characteristics and geological weathering processes are natural sources of these toxic metals in soil. Also, the excessive uses of pesticides and chemical fertilizers, high atmospheric deposition, and wastewater irrigation are external avenues of enriching these heavy metals into agricultural soil [9, 19]. Increased concentration of toxic metals such as copper (Cu), zinc (Zn), arsenic (As), cadmium (Cd) and lead (Pb) are commonly found in the environment of mining activities [15, 42]. The presence of toxic

* Corresponding author.
E-mail address: olusola.kayode@covenantuniversity.edu.ng (O.T. Kayode).

https://doi.org/10.1016/j.heliyon.2022.e08976
Received 20 June 2021; Received in revised form 1 December 2021; Accepted 14 February 2022

metals such as lead (pb), arsenic (As), nickel (Ni), copper (Cu), and cadmium (Cd) at elevated levels in agricultural soils is not only damaging to plant roots but also have health implications in humans [12].

According to Pate and Dauda [35], the vast landmass of northern Nigeria, harnessed, has the potential of an agricultural revolution. To develop a strategy that will bring about sustainable farming practices in this region, an in-depth study of the subsoil features, groundwater potential, and contamination assessment is crucial. The study intends to determine the topsoil features, delineate the aquifer units and identify the heavy metal contaminants in the commercial farm intended for large-scale farming using electrical resistivity and geochemical methods. The data could serve as a guide for future research in the study area and also helpful for agricultural policy and decision-makers to develop effective strategies to improve and manage the soil of the study area.

1.1. Study area

The study area (Figure 1) is the commercial farm of Landmark University Omu-Aran, Kwara State, Nigeria. Landmark University Omu-Aran farm is highly sloppy, with an elevation range of 550 m–575 above sea level. Omu-Aran falls within the southwestern schist belt, bounded by Longitudes 40° 59′47.26" E and 50° 29′41.667" E, and Latitudes 80° 0′ 14.8392" N and 80° 30′15.5664′N. Nigerian schist belt is well-developed in the southwest of Nigeria, trending north-south and extends to Omu-Aran [21, 30]. The underlying rocks in the study area are mostly basement rocks of Precambrian and Cambrian ages and others of Cretaceous and Younger Sediments [30]. Major rocks found in the study area include; granite-gneiss, biotite-granite, and metasediments such as quartzite and quartz-mica schist. Superficial deposits of lateritic boulders overlain the farm area. Omu-Aran in Kwara State, as part of the north-central States of Nigeria, is well known for mining activities and small-scale farming [21]. However, there is no mining activity around the farm area. Kwara State is within the tropical climates and characterized by the low wet and dry seasons with double maxima rainfall. Kwara has an annual rainfall range from 1000 mm to 1500 mm with a uniformly high-temperature range from 25 °C to 30 °C [6, 33]. The soil of Omu-Aran experienced leaching of minerals and nutrients due to high temperature and high seasonal rainfall experienced throughout the year; this makes the soil of the area low in fertility [5].

2. Materials and methods

Five (5) VES and Sixteen (16) 2D electrical resistivity surveys were conducted at Landmark University farm using the Schlumberger and Wenner electrode configurations. All procedures followed the whole theory and applications, as explained by [24, 25]. The field procedures for 1D and 2D resistivity surveys entail inserting some electrodes at structured spacing along a straight line, all electrodes connected to an electric cable which is in turn connected to the ABEM (SAS 1000/4000 series) resistivity meter. Subsequently, current is injected, and the apparent resistivity is deduced from the measured potential difference. The apparent resistivities are then used to delineate the subsurface lithology and geoelectric parameters for 1D and inversed to obtain the 2D resistivity models. The one-dimensional vertical electrical sounding was carried out at five stations on the farm using the Schlumberger array.

In comparison, Wenner array for the 2D resistivity survey was carried out at 16 stations at the research site. Profile orientation maintained a regular north-south direction for 1D and east-west direction for 2D with

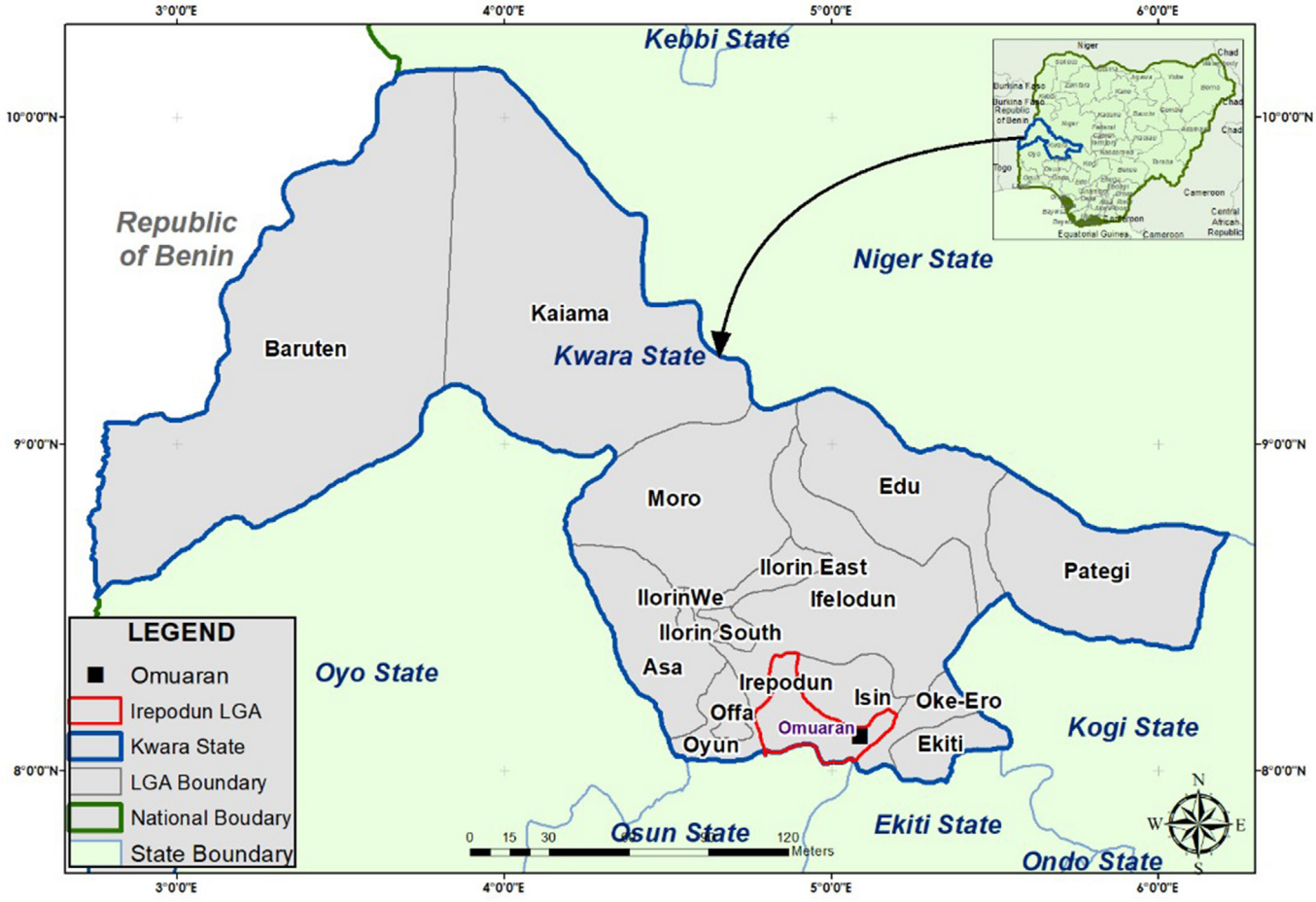

Figure 1. Map showing the study area.

an electrode spacing of 1/2AB is 100–180 m. Schlumberger array, four (4) collinear electrodes were used, with the outer two current electrodes as the source and the two other inner electrodes as the potential or receiver electrodes. Wenner array has an equal spacing of both the current and potential electrodes across the profile. The whole theory and applications of the methods have been documented [23, 25]. Wenner array is an attractive choice for a good vertical resolution envisaged on an agricultural farm, while the Schlumberger has better resolution and is good at probing depths into the subsoil. A reconnaissance survey was done to determine the geology and extent of the area and the field survey was carried out before the planting season. The GARMIN GPS Maps 78 was used for the topographical/elevation data.

2.1. Two-dimensional survey

Similarly, the Sixteen (16) 2D profiles (traverses) were taken on the farmland using the Wenner electrode configurations with the aid of ABEM (SAS 1000/4000 series) resistivity meter. The traverse length was 100 m with 4 m spacing between the traverses (Figure 2). Equal spacing of 1 m between the current electrodes and the potential electrodes was used. Wenner array has a median depth of investigation of approximately 5 m and, therefore, is a good choice for agricultural studies [7].

2.2. Data processing and inversion

The estimates of the resistivity and thicknesses of the delineated layers for the 1D survey were obtained by curve matching the field curves obtained with the Schlumberger master curves. The estimated geoelectric parameters for the five (5) VES points served as initial models for the Win-Resist program used for the computer iteration. The Win-Resist software processed the vertical electrical sounding data to obtain the one-dimensional (1D) resistivity model for each sounded point. The Win-Resist displayed the geoelectric parameters for each sounding point. The observed data are indicated by the cross signs in the resistivity graphs, while the smooth curve shows the computed data (Figure 3). The initial models supplied to the system were used to calculate the computed data, and the misfit between the observed and calculated data was minimized through the iterative process. The resistivity graphs showed the estimated resistivity, thicknesses and depths in each VES point (Figures 3 and 4).

Similarly, the 2D resistivity data were interpreted using the RES2DINV software [26]. The computer program automatically determined the 2D resistivity model of the subsurface for the apparent resistivity data imputed using a nonlinear optimization technique [4]. The resistivity distribution in the subsurface was determined by the inverse model resistivity obtained by the inverted measured apparent resistivity.

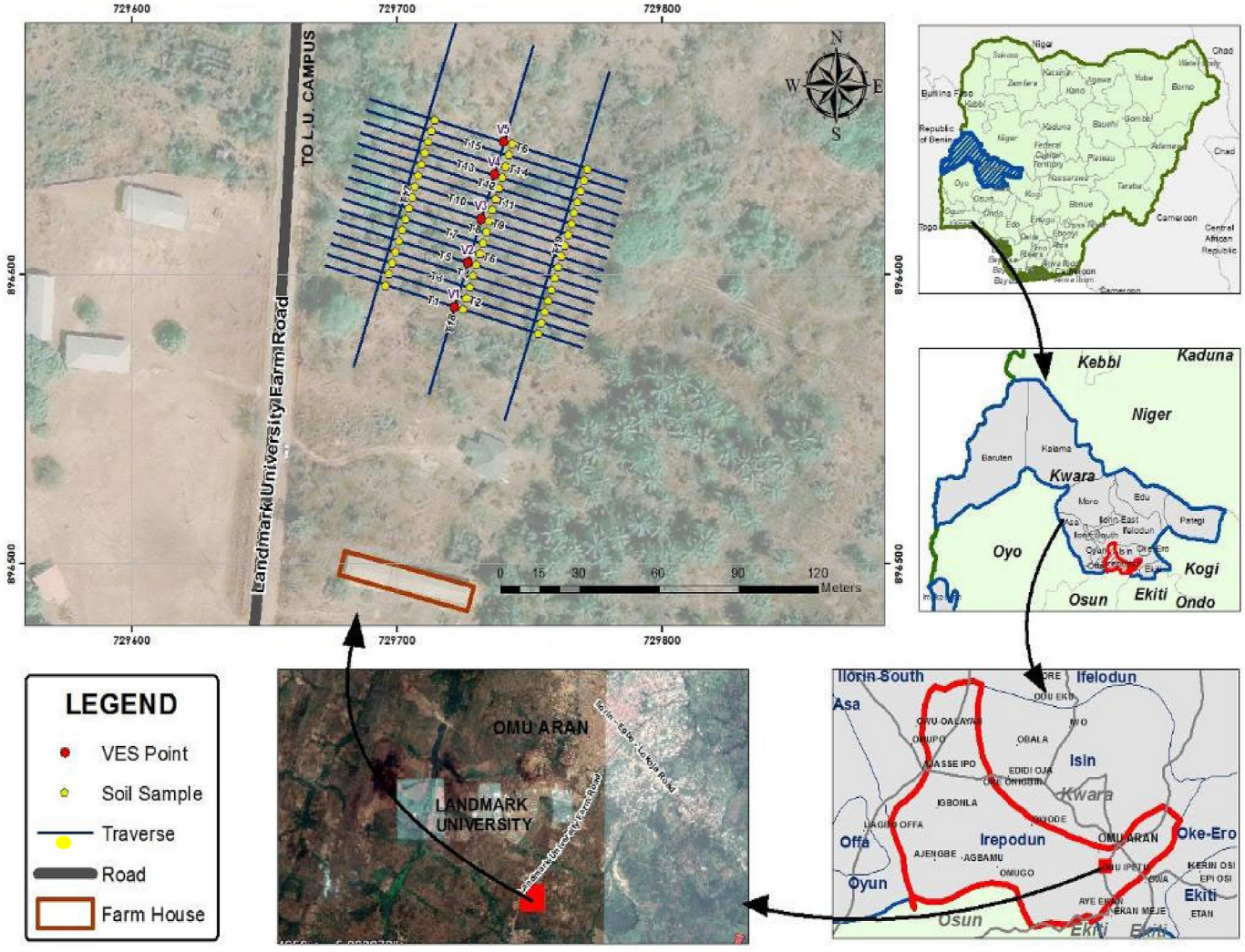

Figure 2. The field layout of the 1D and 2D traverses on the Landmark University farmland.

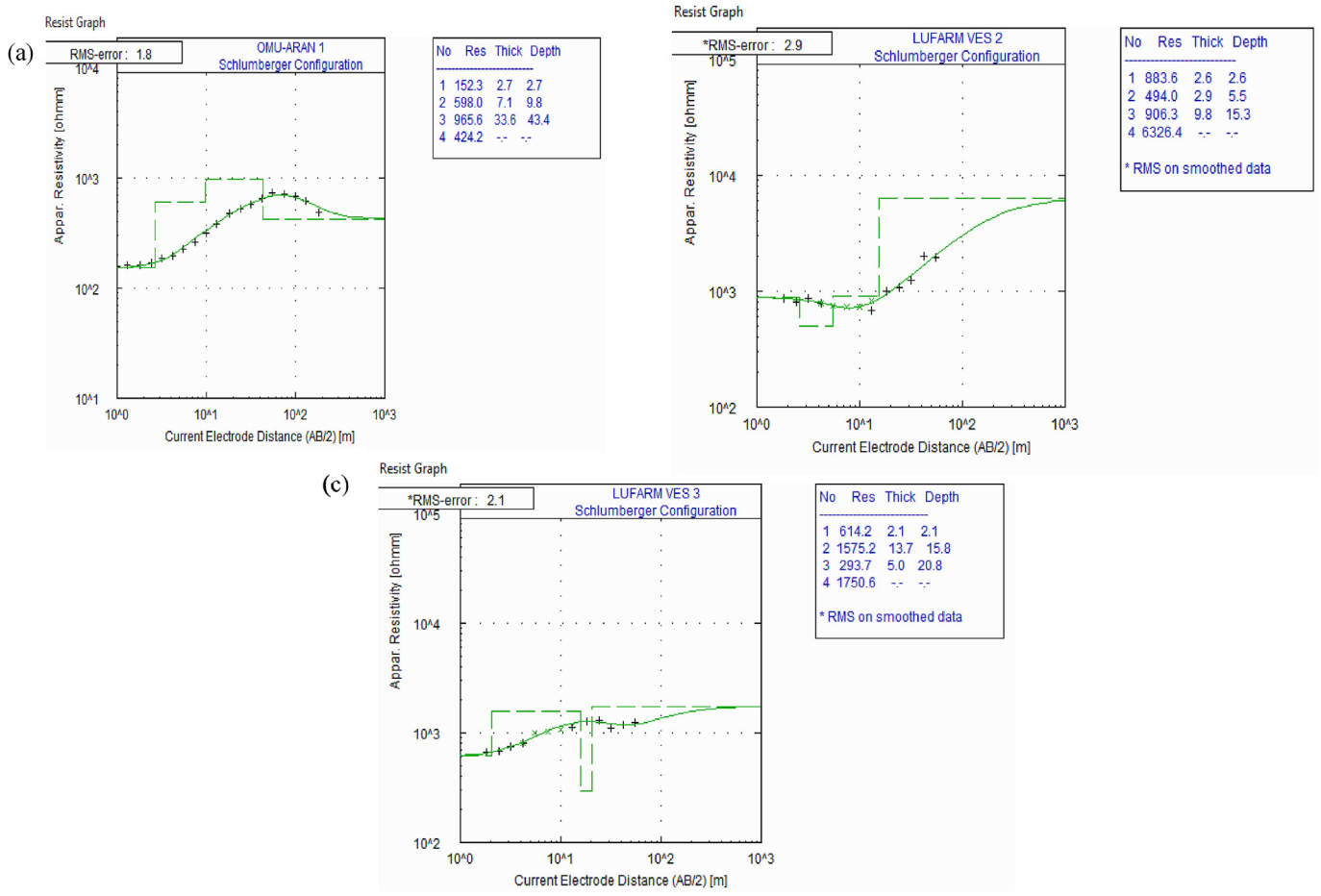

Figure 3. VES curve types: (a) VES1, (b) VES 2, and (c) VES 3 obtained at the LU Omu-Aran farm.

The standard least-square constraints minimized the observed and the calculated apparent resistivity values. The smoothness constraints to the model perturbation vector were applied using Eq. (1):

$$\left[J^T J + \mu\left(f_x f_x^T + f_z f_z^T f\right)\right]\partial = J^T g \tag{1}$$

J is the partial derivatives of Jacobian matrix and the transpose to J^T, μ is the damping factor, f^x and f^z are the horizontal flatness and vertical flatness respectively, ∂ is the model perturbation vector, and g is the discrepancy factor. The inversion was also done with a standard Gauss-Newton optimization having a 0.05 convergence. The optimization of the damping factor was used to reduce the number of iterations required for convergence giving the least root mean square (RMS) error. Topography models were created by imputing the topographic data points into the 2D inversed models.

2.3. Geochemical method

Eight (8) soil samples from the farm location were collected in clean well-labeled polythene bags with the aid of a hand trowel at a depth of

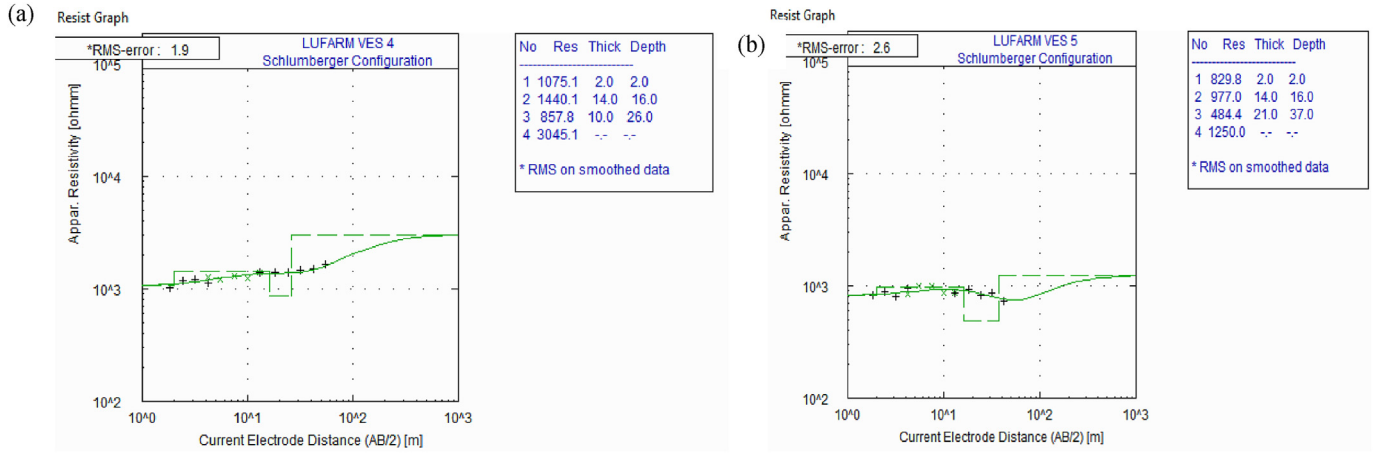

Figure 4. VES curve types showing: (a) VES 4, and (b) VES 5 obtained at the LU Omu-Aran farm.

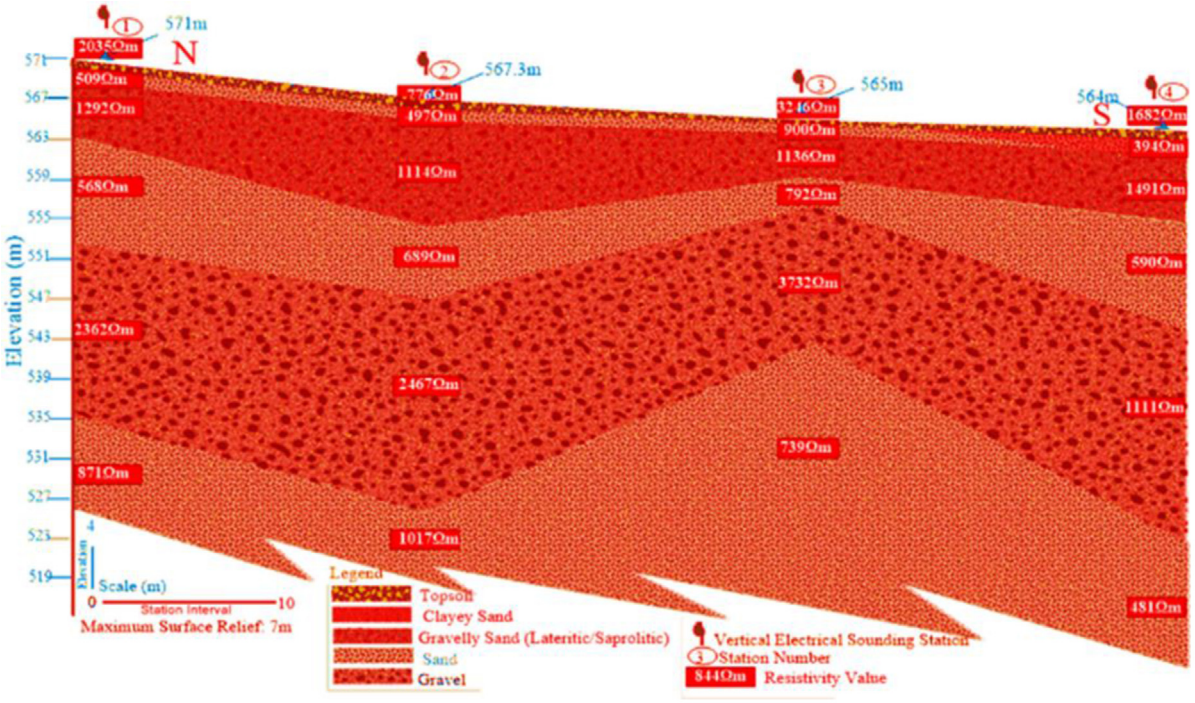

Figure 5. Geoelectric section of the subsoil of Landmark University farm Omu-Aran.

40–60 cm (topsoil)) at the farm site. Soil samples were dried in the oven at 40 °C; agglomeration was removed by hammering, after which samples were homogenized in porcelain mortal. Multi-acid digestion with perchloric and hydrofluoric acid (HF) was used to determine the element concentration for all the soil samples. The total digestion of soil samples was carried out by using the analytical packet (MA250) or inductively coupled plasma mass spectrometry (ICPMS) at the Bureau Veritas Laboratory Vancouver, Canada. A 0.25 g split of each soil sample was heated to fuming in a triple acid (HNO_3 $-HClO_4$ $-HF$) and was after that dried. The residue was dissolved in 50% HCl solution. Strong oxidising agents totally removed organic matter (HNO_3 *and* $HClO_4$), while the dissolution of silicates was done by using HF, this allows the near-total dissolution of the mineral fraction. The measurement detection limit (MDL) for the toxic metals analysed ranged from 0.01 mg/kg to 0.2 mg/kg. The analysis followed standard procedures using STD OREAS25A and STD OREAS45E as standard reference materials [16, 43]. L1 - L8 represents the soil samples from the study area.

Contamination factor (Cf) and pollution load index (PLI) were used to assess the degree of contamination in the study area. The contamination factor (Cf) was calculated using Eq. (2):

$$Cf = \frac{C_n}{B_n} \tag{2}$$

where C_n is the concentration of metals and B_n is the background values/crustal average value of element. Cf $\leq$ 1 is low contamination, 1 $<$ Cf $\leq$ 3 is moderate contamination and Cf $>$ 3 is high contamination. Previous researchers have used pollution load index (PLI) which is also known as Tomlinson's pollution index and the Nemerow integrated pollution load index (NIPI) to assess the overall pollution status for soil samples [27, 28, 41]. The PLI was calculated using Eq. (3):

$$PLI = \sqrt[n]{Cf_1} \times Cf_2 \ldots \times Cf_n \tag{3}$$

PLI is pollution load index, n is the number of samples, Cf_n is the Cf of metal n. The Nemerow integrated pollution load index (NIPI) was calculated using Eq. (4):

$$NIPI = \sqrt{0.5\left(I_{mean}^2 + I_{max}^2\right)} \tag{4}$$

Table 1. Geoelectric sections of the study area.

VES no	Layer	Resistivity (Ωm)	Thickness (m)	Depth (m)	Inferred Lithology
1	1	152.3	2.7	2.7	Topsoil (Clayey)
	2	598.8	7.1	9.8	Upper Saprolite
	3	965.6	33.6	43.4	Fractured Basement
	4	424.2	-	-	Fractured basement
2	1	883.6	2.6	2.6	Topsoil (Stone zone)
	2	494	2.9	5.5	Upper Saprolite
	3	906.3	9.8	15.3	Lower Saprolite
	4	6326.4	-	-	Fresh Basement
3	1	614.2	2.1	2.1	Topsoil (Stone zone)
	2	1575.2	13.7	15.8	Upper Saprolite
	3	293.7	5	20.8	Lower Saprolite
	4	1792.6	-	-	Fractured Basement
4	1	1075.1	2	2	Topsoil (Stone zone)
	2	1440.1	14	16	Upper Saprolite
	3	857.8	10	26	Lower Saprolite
	4	3045.1	-	-	Fresh Basement
5	1	829.8	2	2	Topsoil (Stone zone)
	2	977	14	16	Upper Saprolite
	3	484.4	21	37	Fractured Unit
	4	1250	-	-	Fractured Basement

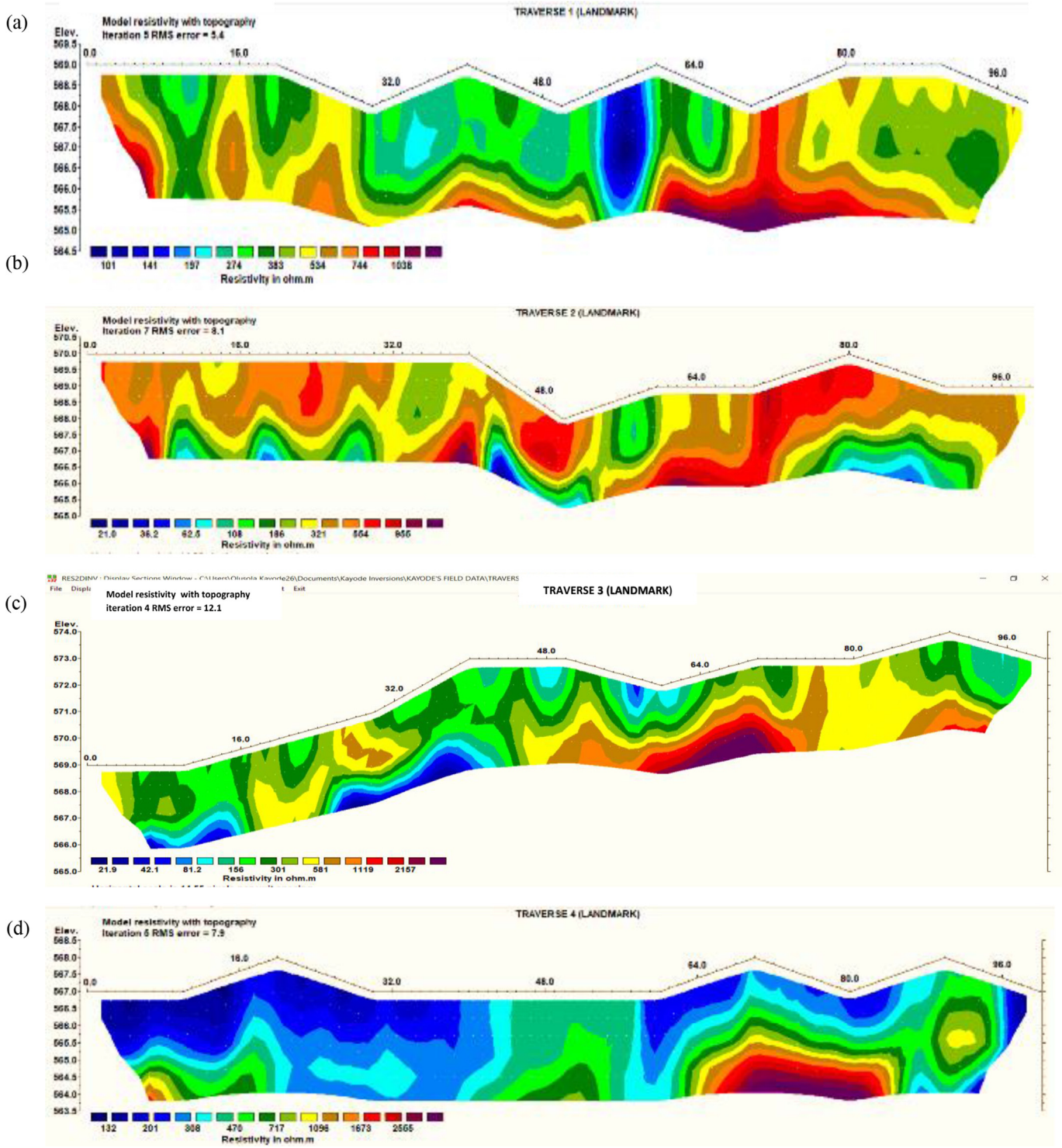

Figure 6. 2D resistivity inverse model for: (a) Traverse 1, (b) Traverse 2, (c) Traverse 3; and (d) Traverse 4 at Landmark University farm.

The mean value of all CF is I_{mean}, and the maximum value of the mean is I_{max}.

3. Results and discussion

3.1. Vertical electrical soundings (VES) or ID data interpretation

Resistivity contrast among subsoil layers and the information from the local geology of the study area were used to interpret and identify the lithology as previously noted by Carriere etal., Keller and Frischnecht [13] and [22]. The three-layer curve type displayed by the VES curves (Figures 3 and 4) is the primary classification of resistivity curves peculiar to the basement complex terrain. The geoelectric sections of the subsurface features at varying depths of sounding points in the studied site are presented in Figure 5. The summary of the VES interpretation carried out at the study area is shown in Table 1. The four (4) VES stations have indicated that the topsoil (stone zone) of the study site is heterogeneous having a mixture of clayey sand, gravelly and sandy soils with resistivity ranging from 152 Ωm to 1075 Ωm. The average resistivity of the topsoil delineated from all the layers is 711 Ωm with thickness

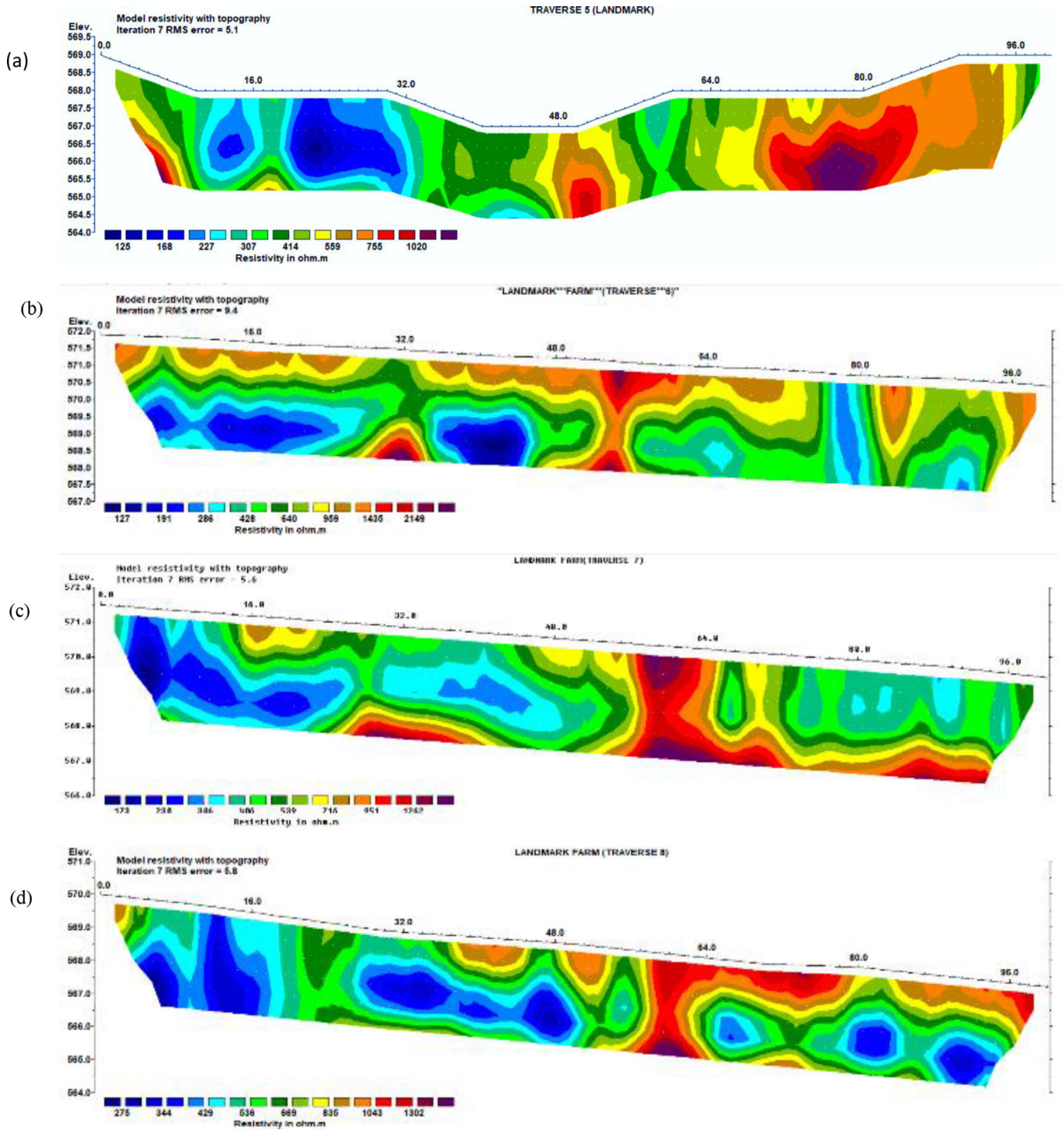

Figure 7. 2D resistivity inverse models for: (a) Traverse 5, (b) Traverse 6, (c) Traverse 7, and (d) Traverse 8 at Landmark University farm.

ranging from 2.0 to 2.7 m and average thickness of 2.3 m. This layer covered the upper root zone of several significant crops (maize, beans, rice, okra, millet). The second layer is the weathered layer that is, the upper and lower saprolites (sandy/lateritic gravelly sand) having resistivity ranging from 495 Ωm to 1575 Ωm, while the third and fourth layer are the fractured unit and fresh basement respectively.

The result has indicated that the clayey sand, the gravelly, and sandy soils are the major constituents of the site in Landmark University farm with resistivity ranging from 152 Ωm to 3045 Ωm (Table 1). The average thickness of the weathered layer may not support groundwater yield [32]. Therefore, the fractured zone with massive sand body at depth ˃37 m is delineated as an aquiferous zone at the farm site. The previous study in Landmark University community has delineated the weathered basement and fractured basement at depth ˃30m above the subsurface as the aquiferous zones having potential for groundwater exploitation [31]. The high resistivity (3045–6326 Ωm) of the fresh basement in most of the VES stations indicate a negligible permeability with a very low porosity. The local geology and available information were used to infer the lithologies

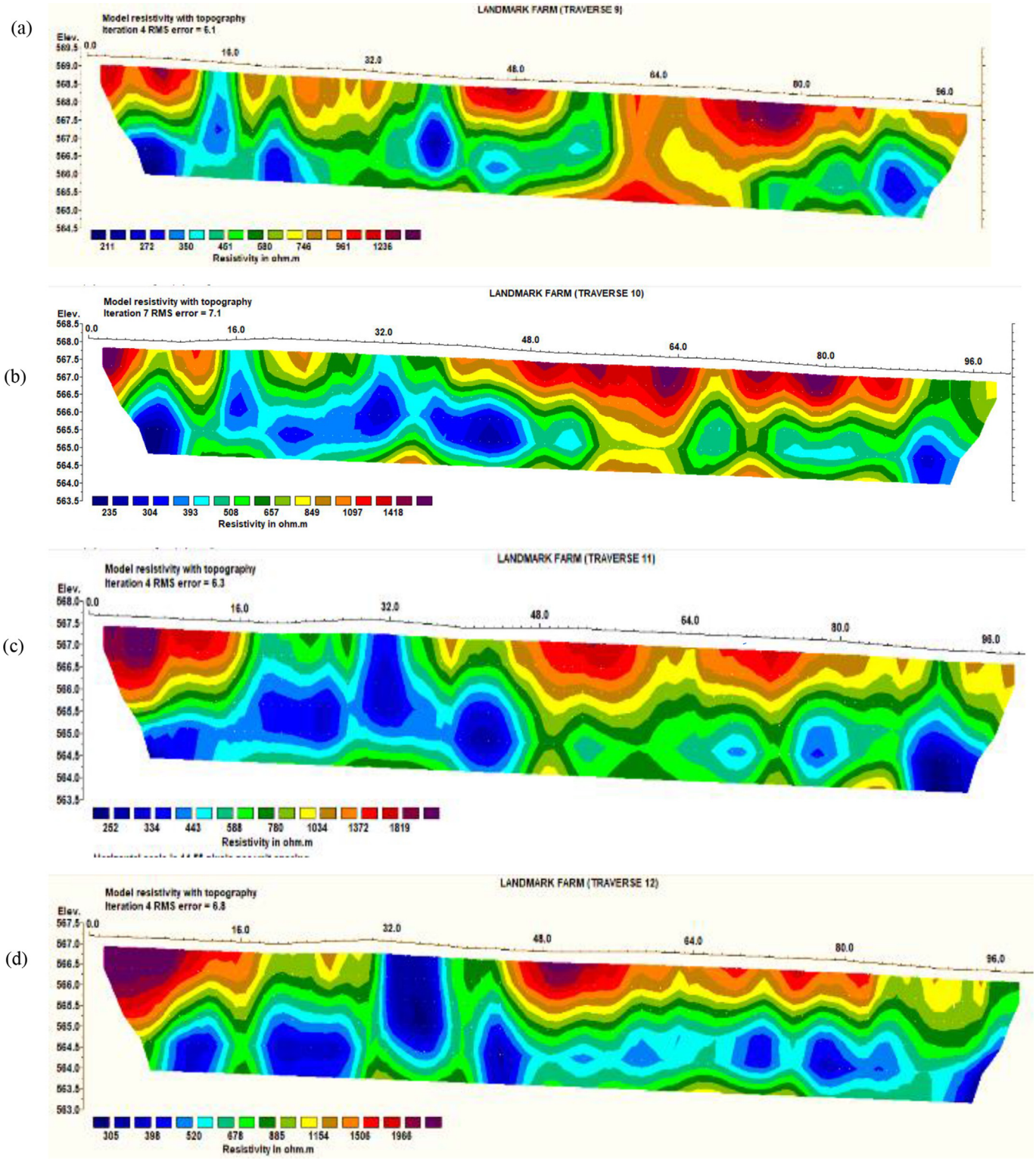

Figure 8. 2D resistivity inverse models for: (a) Traverse 9, (b) Traverse 10, (c) Traverse 11, and (d) Traverse 13 at Landmark University farm.

of interpreted layers. The identified curve types for Omu-Aran farm are the HK curve types (bowl - bell curves). The different VES curve types have been discussed by several authors [1, 40].

3.2. Interpretation of 2D resistivity traverses

Figures 6, 7, 8, and 9 showed the inverse resistivity models for all the traverses at the Landmark University farm. Useful information about the subsoil condition along the profile of interest in the study area was provided by the application of 2D electrical resistivity imaging. The resistivity values for all the traverses ranged from 21.0 to 3145 Ωm and the depth of investigation covered the upper root zone ≥2. High resistivity (>300) values generally characterized the inverse resistivity models at the farm. However, for all the traverses, patches of low resistivity (<100) are observed at depths below 2m. The high resistivity values observed at the study area were attributed to sandy and gravelly sand constituents in

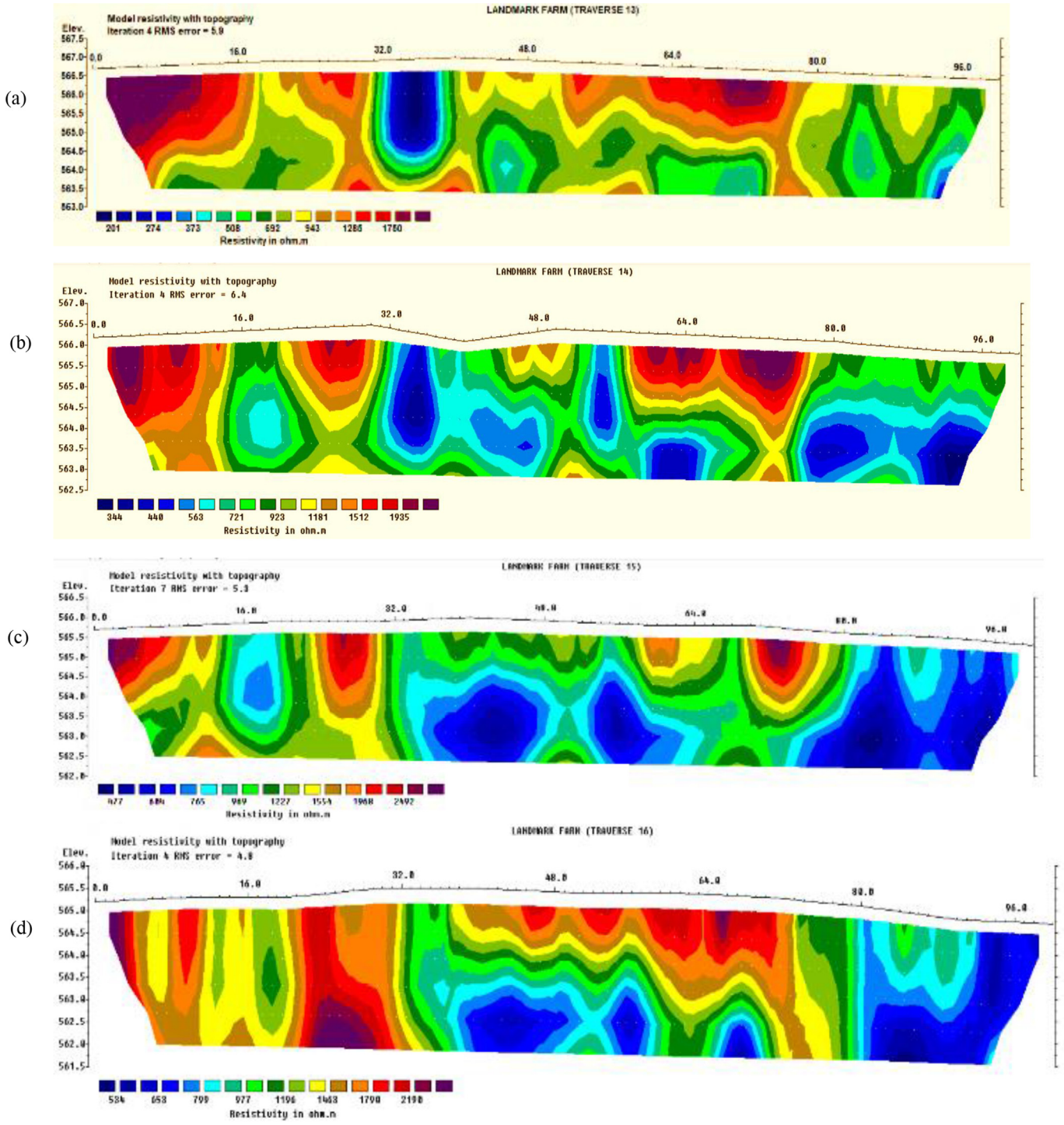

Figure 9. 2D Inverse models at Landmark University farm for: (a) Traverse 13, (b) Traverse 14, (c) Traverse 15, and (d) Traverse 16.

the farm, while the low resistivity (<100) values observed in Figures 4b and 4c is indicative of clayey soil. The change in resistivity values observed from the inverse resistivity models is consequent to the differences in the degrees of compaction, organic matter and moisture content. The mixture of clayey sand, gravelly sand and sandy in varying proportion is evident of the heterogeneous nature of the topsoil, as observed in the site at Landmark University farm. Gravelly sand and sandy soil are the dominant soil delineated at Landmark University farm from the geoelectrical analysis. The inability of sandy soil to retain nutrient is a significant limitation of its crop production capacity [10]. Also, sandy gravelly soils generally have poor water holding capacity; therefore, for sustainable farming practices in areas with such soil type, irrigation is the only alternative.

3.3. Geochemical analysis

The geochemical analysis results of toxic elements in the soil of the study area are presented in Table 2. The toxic metals identified in the study area include arsenic (As), cadmium (Cd), cobalt (Co), chromium (Cr), copper (Co), nickel (Ni), manganese (Mn), lead (Pb) and zinc (Zn).

Table 2. Toxic elements concentration (mg/kg) in Landmark University farm (n = 8).

Elements	Crustal Average (1964)	L1	L2	L3	L4	L5	L6	L7	L8
As	1.5	4.3	2.6	4.2	4.6	4.6	4.3	2.0	1.2
Cd	0.1	0.01	0.01	0.01	0.01	0.01	0.01	0.12	0.09
Co	17.0	6.10	5.10	5.5	6.6	6.20	6.50	17.4	9.70
Cr	83.0	56.0	55.0	60.0	67.0	72.0	71.0	58.0	38.0
Cu	25.0	19.3	16.4	22.2	22.0	21.2	23.9	24.5	16.8
Mn	600	360	292	402	329	393	323	1137	554
Ni	44.0	21.4	17.3	21.9	25.0	21.8	26.1	19.7	12.3
Pb	17.0	18.46	15.58	19.37	19.73	19.22	21.3	49.9	36.5
Zn	71.0	28.6	23.2	29.5	30.1	28.7	34.1	156.9	96.0

N/A-Not Available.

Table 3. Contamination factor at Landmark University farm.

Toxic elements	Contamination Factor (Range)	Contamination Factor	Interpretation
As	0.80–2.87	2.33	Low to Moderate Contamination
Cd	0.10–0.20	0.34	Low to Moderate Contamination
Co	0.30–1.02	0.46	Low to Moderate Contamination
Cr	0.46–0.87	0.72	Low Contamination
Cu	0.66–1.29	0.88	Low to Moderate Contamination
Ni	0.28–0.6	0.47	Low Contamination
Mn	0.49–1.90	0.79	Low to Moderate Contamination
Pb	0.92–2.93	1.47	Low to Moderate Contamination
Zn	0.33–2.21	0.75	Low to Moderate Contamination

Table 4. Pollution load index (PLI and NIPI) at Landmark University farm.

Toxic elements	*Pollution load index (PLI)*	Nemerow integrated pollution index (NIPI)	Interpretation
As	2.12	0.93	Unpolluted to Moderate Pollution
Cd	0.18	0.21	Unpolluted
Co	0.42	0.79	Unpolluted
Cr	0.71	0.79	Unpolluted
Cu	0.83	0.91	Unpolluted
Ni	0.46	0.53	Unpolluted
Mn	0.71	0.71	Unpolluted
Pb	1.36	2.33	Moderate Pollution
Zn	0.58	1.64	Unpolluted to Moderate Pollution

Tables 3 and 4 showed the contamination factor, pollution load index (PLI) and Nemerow integrated pollution index (NIPI) at Landmark University farm.

The contamination factor of toxic elements in the study area indicated low to moderate contamination. As, Pb, Mn, Co, Cd, and Zn are within low to moderate contamination, while Cr and Ni are in low contamination (Table 3). Arsenic (As) concentration was the highest contaminant in the site at Landmark University farm, having a contamination factor of 2.33. The pollution index of the toxic elements showed a descending order of As > Pb > Cu > Cu > Mn > Zn > Cr > Ni > Co > Cd (Table 4).

The pollution load index (PLI) and Nemerow integrated pollution index at the farm site indicated an unpolluted to moderately polluted soil in the farm area. Table 4 showed a moderate risk of arsenic at the study site. The low and moderate concentrations of the identified toxic elements in the farmland make the farm suitable for farming activities. The results also indicate that no recent mining activity is noticed around the farm site. However, management practices should be encouraged as higher concentrations of these toxic elements threaten toxicity to plants and ecosystems in the environment.

4. Conclusions

The geoelectrical resistivity method has identified subsoil features for sustainable and precision agriculture with several data analyses. The dataset identifies soil types, lithology variations with depths in the subsurface. It also showed the subsoil resistivity variations used to delineate the degree of water saturation (water content) and the arrangement of voids (pore size distribution and porosity). Results have shown that sandy and gravelly sand soil are prevalent in Landmark University farmland, Omu-Aran, and sandy and gravelly soils are deficient in nutrients. However, frequent fertilization can improve sandy soils to enhance agricultural production in the area. The toxic elements identified in the farm indicate sources are majorly from the natural processes of weathering due to the low to moderate contamination of these elements in the soil of the study area. Therefore, chemical and organic fertilizers should be added to soil in required proportion at the farm to reduce the accumulation of toxic elements detrimental to crop production and human health. This study can assist agricultural policymakers and researchers in the field of soil science and environmental studies. Also, decision-makers can use the information for planning and designing large agricultural fields for sustainable farming. Geochemical analysis can be carried out on soil samples of this area to ascertain the fertility status of the soil before the planting season.

Declarations

Author contribution statement

O. T Kayode: Conceived and designed the experiments; Performed the experiments; Analyzed and interpreted the data; Contributed reagents, materials, analysis tools or data; Wrote the paper.

A. P Aizebeokhai: Performed the experiments; Analyzed and interpreted the data.

A. M Odukoya: Contributed reagents, materials, analysis tools or data.

Funding statement

This research did not receive any specific grant from funding agencies in the public, commercial, or not-for-profit sectors.

Data availability statement

Data will be made available on request.

Declaration of interests statement

The authors declare no conflict of interest.

Additional information

No additional information is available for this paper.

Acknowledgements

The authors wish to thank the Covenant University Management for providing the enabling environment for this research through Centre for Research, Innovation and Discovery (CUCRID), Covenant University.

References

[1] A.P. Aizebeokhai, K.D. Oyeyemi, F.R. Noiki, B.I. Etete, A.U.E. Arere, U.J. Eyo, V.C. Ogbuehi, Geoelectrical resistivity datasets for subsurface characterization and aquifer delineation in Iyesi, Southwestern Nigeria, Data Brief 15 (2017) 828–832.
[2] A.P. Aizebeokhai, K.D. Oyeyemi, Geoelectrical characterisation of basement aquifers: the case of Iberekodo, southwestern Nigeria, Hydrogeol. J. 26 (2018) 651–664.
[3] A.P. Aizebeokhai, K.D. Oyeyemi, O.T. Kayode, Assessment of soil petrophysical parameters using electrical resistivity tomography (ERT) and induced polarization techniques, Res. J. Appl. Sci. 10 (9) (2015) 479–485.
[4] A.P. Aizebeokhai, 2D and 3D geoelectric resistivity imaging: theory and field design, Sci. Res. Essays 5 (23) (2010) 3592–3605. http://www.academicjournals.org/SRE.
[5] B.S. Ajadi, A. Adeniyi, M.T. Afolabi, Impact of climate on urban agriculture: case study of Ilorin city, Nigeria, Global J. Hum. Soc. Sci. 11 (1) (2011) 1–7.
[6] T.D. Akpenpuun, Climate and grain crops yield in Kwara state, Nigeria, J. Emerg. Trends Eng. Appl. Sci. 4 (5) (2013) 737–774.
[7] B.J. Allred, M.R. Ehsani, J.J. Daniels, General considerations for geophysical methods applied to agriculture, in: B.J. Allred, J.J. Daniels, M.R. Ehsani (Eds.), Hand-Book of Agricultural Geophysics (3-16, CRC Press, Taylor and Francis Group, Boca Raton, Florida, 2008.
[8] B. Amato, G. Basso, G. Celano, G. Bitella, R. Morelli, R. Rossi, In situ detection of tree root distribution and biomass by multielectrode resistivity imaging, Tree Physiol. 28 (10) (2008) 1441–1448.
[9] M. Amir, H. Bhuiyan, S.C. Karmaker, M. Bodrud-Doza, M.A. Rakib, B.B. Saha, Enrichment, sources and ecological risk mapping of heavy metals in agricultural soils of Dhaka district employing SOM, PMF and GIS methods, Chemosphere 263 (2021) 1–14.
[10] S.D. Basga, J.P. Ngyetnkam, Fertilizing effect of swelling clay minerals on the growth and yield of bean "*Phaseolus vulgaris*" on the sandy ferruginous soils from Mafa Tcheboa (North Cameroun, Central Africa), Int. J. Phys. Soc. Sci. 5 (1) (2015) 10–24.
[11] B. Basso, M. Amato, R. Bitella, R. Rossi, A. Kravchenko, L. Sartori, L.M. Carvahlo, J. Gomes, Two dimensional spatial and temporal variations of soil physical properties in tillage systems using electrical resistivity tomography, Agron. J. 102 (2010) 440.
[12] J. Briffa, E. Sinagra, R. Blundell, Heavy metal pollution in the environment and their toxicological effects on humans, Heliyon 6 (9) (2020), 8e04691, 1-26.
[13] S.D. Carriere, J. Ruffault, F. Pimont, C. Doussan, G. Simoni, K. Chalikakis, J.M. Limousin, I. Scotti, F. Courdier, C.B. Cakpo, H. Davi, N.K. Martin-St Paul, Impact of local soil and subsoil conditions on inter-individual variations in tree responses to drought: insights from Electrical Resistivity Tomography, Sci. Total Environ. 698 (2020) 1–10.
[14] G. Celano, A.M. Palese, E. Martorella, N. Vignozzi, C. Xiloyannis, Evaluation of soil water content in tilled and cover-cropped olive orchards by the geoelectrical technique, Geoderma 163 (2011) 163–170.
[15] L. Demkova, T. Jezny, L. Bobulska, Assessment of spoil heavy metal pollution in a former mining site-befor and after the end of mining activities, Soil Water Res. 12 (2) (2017) 1–10.
[16] C. Finch, R. Roldan, L. Walsh, J. Kelly, S. Amor, Analytical Methods for Chemical Analysis of Geological Materials, Government of New foundland and Labrador, Department of Natural Resources, 2018, pp. 1–24. Geological Survey, Open File NFLD (3316).
[17] S.A. Ganiyu, O.T. Olurin, M.A. Oladunjoye, B.S. Badmus, Investigation of soil moisture content over a cultivated farmland in Abeokuta Nigeria using electrical resistivity methods and soil analysis, King Saud Univer. Sci. 32 (1) (2020) 811–821.
[18] I.C. Garre, C. Wongleecharoen, K. Hussain, W. Omsunrarn, T. Kongkaew, T. Hilger, J. Diels, J. Vanderborght, Can we use electrical resistivity tomography to measure root zone dynamics in fields with multiple crops? Proc. Environ. Sci. 19 (2013) 403–410.
[19] W. Hu, H. Wang, L. Dong, B. Huang, O.K. Borggaard, H.,C.B. Hansen, Y. He, P.E. Holm, Source identification of heavy metals in peri-urban agricultural soils of southeast China: an integrated approach, Environ. Pollut. 237 (2018) 650–661.
[20] X. Jia, D. O'Connor, D. Hou, Y. Jin, G. Li, C. Zheng, Y.S. Ok, D.C.W. Tsang, J. Luo, Groundwater depletion and contamination: spatial distribution of groundwater resources sustainability in China, Sci. Total Environ. 672 (2019) 1–30.
[21] J.S. Kayode, N.S.M. Namawi, H.M. Baioumy, B.A. Khiruddin, Delineation of the subsurface geological structures of Omu-Aran area, southwestern Nigeria using aeromagnetic data, AIP Conf. Proc. 1657 (1) (2015), 040012.
[22] S. Keller, N. Frischnecht, An interactive computer/graphic-display-terminal system for interpretation of resistivity soundings, Geophys. Prospect. 23 (1970) 449–458.
[23] M.H. Loke, Electrical resistivity surveys and data interpretation, in: H. Gupta (Ed.), Solid Earth Geophysics Encyclopaedia, second ed.Electrical & Electromagnetic, Springer-Verlag, 2011, pp. 276–283.
[24] M.H. Loke, RES2DINV Software (Geotomo Software) User's Manual, 2010.
[25] M.H. Loke, Tutorial: 2-D and 3-D Electrical Imaging Surveys, 2001.
[26] M.H. Loke, R.D.1 Barker, Rapid least-squares inversion of apparent resistivity pseudosections using a quasi-Newton method, Geophys. Prospect. 44 (1996) 131–152.
[27] X. Lu, X. Zhang, L.Y. Li, H. Chen, Assessment of metals pollution and health risk in dust from nursery schools in Xi'an, China, Environ. Res. 128 (2014) 27–34.
[28] N.L. Nemerow, Stream, Lake, Estuary and Ocean Pollution, first ed., Van Nostrand Reinhold Publishing Company, New York, 1985, p. 472.
[29] W. Nijland, M. Meijde, M. Addink, M. de jong Steven, Detection of soil moisture and vegetation water abstraction in a Mediterranean natural area using Electrical Resistivity Tomography, Catena 81 (2010) 209–216.
[30] N.J. Obaje, Geology and Mineral Resources of Nigeria, Springer, Berlin, 2009, pp. 1–221.
[31] E. Odeyemi, D.A. Oluwafemi, O. Olaonipekun, Geophysical investigation of aquifer layer of Landmark University community, Omu-Aran, Nigeria using electrical resistivity method, J. Eng. Appl. Sci. 14 (12) (2019) 4285–4289.
[32] M.A. Oladunjoye, A. Adefehinti, I.A. Korode, Use of two dimensional electrical resistivity imaging to assess groundwater potential in the basement rock of Gbongudu Community, Southwestern Nigeria, Online J. Earth Sci. 12 (2018) 8–29.
[33] R.M. Olanrewaju, Climate and the growth cycle of yam plant in the Guinea Savanna ecological zone of Kwara State, Nigeria, J. Meteorol. Clim. Sci. 7 (2009) 43–48.
[34] C.M. Paglis, Application of electrical resistivity tomography for detecting root biomass in coffee trees, J. Geophys. Int. (2013) 1–6.
[35] U.A. Pate, S. Dauda, Media and socio-economic development in northern Nigeria, Malays. J. Commun. 29 (1) (2013) 1–19.
[36] A. Samouëlia, I. Cousin, A. Tabbagh, A. Bruand, G. Richard, Electrical resistivity in soil science: a review, Soil Tillage Resour. 83 (2005) 173–193.
[37] S. Senthilkumar, B. Gowtham, K. Srinivasamoorthy, S. Gopinath, Hydrogeochemical delineation of groundwater fitness for drinking and agricultural utilities in Thiruvallur district, South India, Arabian J. Geosci. 14 (526) (2021).
[38] A. Shakoor, Z.M. Khan, H.U. Farid, M. Sultan, I. Ahmad, N. Ahmad, M.H. Mahmood, M.U. Ali, Delineation of regional groundwater vulnerability using DRASTIC model for agricultural application in Pakistan, Arabian J. Geosci. 13 (2020) 195.
[39] D. Srayeddin, C. Doussan, Estimation of the spatial variability of root water uptake of Maize and Sorghum at the field scale by electrical resistivity tomography, Plant Soil 319 (1–2) (2009) 185–207.
[40] L.A. Sunmonu, T.A. Adagunodo, O.G. Bayowa, A.V. Erinle, Geophysical mapping of the proposed Osun State housing estate, Olupona for subsurface competence and groundwater potential, J. Basic Appl. Res. 2 (2) (2016) 27–47. ISSN 20413-7014.
[41] D.C. Tomlinson, J.G. Wilson, C.R. Harris, D.W. Jeffrey, Problems in the assessment of heavy metals levels in estuaries and the formation of pollution index, Helgol. Mar. Res. 33 (1980) 566–575.
[42] A.Z. Tun, P. Wongsasuluk, W. Siriwong, Heavy metals in the soils of small-scale gold mining sites in Myanmar, J. Health Pollut. 10 (27) (2020) 1–8.
[43] S.C. Wilschefski, M.R. Baxter, Inductively coupled plasma mass spectrometry: introduction to analytical aspects, Clin. Biochem. Rev. 40 (3) (2019) 115–133.
[44] W.Y. Xia, Y.J. Du, F.S. Li, G.L. Guo, X.L. Yan, C.P. Li, A. Arulrajah, F. Wang, S. Wang, Field evaluation of a new hydroxyapatite-based binder for ex-situ solidification/stabilization of a heavy metal contaminated site soil around a Pb-Zn smelter, Construct. Build. Mater. 210 (2019) 278–288.
[45] R. Xiao, F. Shen, J. Du, R.H. Li, A.,H. Lahori, Z.Q. Zhang, Screening of native plants from wasteland surrounding a Zn smelter in Feng County China, for phytoremediation, Ecotoxicol. Environ. Saf. 162 (2018) 178–183.